

## Load-Based Power Saving for Downlink Non-Real-Time Traffic in LTE-TDD

Chun-Chuan Yang<sup>a\*</sup>, Jeng-Yueng Chen<sup>b</sup>, Yi-Ting Mai<sup>c</sup> and Zheng-Ying Pan<sup>a</sup>

<sup>a</sup>Department of Computer Science & Information Engineering,  
National Chi Nan University, Puli, Taiwan

<sup>b</sup>Department of Information & Networking Technology,  
Hsiuping University of Science & Technology, Taichung City, Taiwan

<sup>c</sup>Department of Sport Management, National Taiwan University of Sport,  
Taichung City, Taiwan

\*Corresponding Author: ccyang@csie.ncnu.edu.tw

### ABSTRACT

Long Term Evolution (LTE) is a 4G wireless broadband technology developed by the Third Generation Partnership Project (3GPP). LTE uses two different types of radio links, one for downlink (from the eNodeB or base station to the UE or user equipment), and one for uplink (from UE to eNodeB). Two duplex modes namely frequency division duplex (FDD) and time division duplex (TDD) are defined in LTE for transmission in both directions simultaneously. Power saving mechanisms for LTE-FDD were proposed in the authors' previous work. Applicability of the previously proposed mechanisms to LTE-TDD is investigated in this paper, and the idea of virtual time as well as the mapping mechanism from virtual time to real time for different TDD configurations is proposed. Simulation study demonstrates the benefit of the proposed mechanisms in terms of power saving efficiency in comparing with the standard-based mechanism.

**Keyword:** LTE, TDD, DRX, Power Saving.

### 1. Introduction

As a major 4G system, *Long-Term Evolution (LTE)* (3GPP, 2008) and its enhancement namely *LTE-Advanced (LTE-A)* (3GPP, 2011) are being deployed around the world and phasing out 2G and 3G cellular radio methods. LTE is designed to work with a variety of different bandwidths and to deliver a peak data rate of 100 Mbps in the downlink and 50 Mbps in the uplink, in which the *uplink* is defined for the transmission from the user equipment (denoted by *UE*) to the base station (denoted by *eNodeB*), and the *downlink* is defined for the transmission from eNodeB to UE. In order to be able to transmit in both directions, a UE or eNodeB must have a duplex scheme. There are two forms of duplex defined in LTE, namely *frequency division duplex (FDD)* and *time division duplex (TDD)*.

FDD implies that downlink (DL) and uplink (UL) transmission take place in different, sufficiently separated, frequency bands. In the case of TDD, there is a single frequency band only and uplink and downlink transmissions are separated in the time domain on a cell basis. Different asymmetries in terms of the amount of resources, i.e. subframes, allocated for uplink and downlink transmission respectively are provided through the seven different DL/UL configurations within a radio frame (10ms) as displayed in Table 1. The switch between DL and UL occurs in the special subframe (denote by S in Table 1), which is split into three parts: a downlink part (DwPTS), a guard period (GP), and an uplink part (UpPTS).

Table 1. TDD Configuration

DL/UL Configuration	Subframe number									
	0	1	2	3	4	5	6	7	8	9
0	D	S	U	U	U	D	S	U	U	U
1	D	S	U	U	D	D	S	U	U	D
2	D	S	U	D	D	D	S	U	D	D
3	D	S	U	U	U	D	D	D	D	D
4	D	S	U	U	D	D	D	D	D	D
5	D	S	U	D	D	D	D	D	D	D
6	D	S	U	U	U	D	S	U	U	D

Note: D: DL subframe, U: UL subframe, S: Special subframe

The DwPTS can be treated as a DL subframe that can be used to transmit a smaller amount of data than a regular subframe. The UpPTS, however, is not used for data transmission due to the very short duration. Instead, it can be used for channel sounding or random access. It can also be left empty, in which case it serves as extra guard period.

In a dynamic TDD system, the DL/UL configuration can be changed based on the traffic load, which leads to the performance issue of Hybrid Automatic Repeat Request (HARQ) operation. HARQ signaling design in LTE-TDD in order to reduce HARQ round-trip time was addressed in the literature (Wang et al., 2014; Lu et al., 2012; Sheu et al., 2013). In addition, efficient resource allocation in LTE-TDD was addressed in some research works (Li et al., 2014; Ji et al., 2013, Brown & Khan, 2012). To the authors' knowledge, the focus of the paper, energy-saving in LTE-TDD, has not been addressed in the literature.

The authors have been researching power saving mechanisms in wireless communication systems for some years. The idea of *Load-Based Power Saving (LBPS)* and associated schemes were proposed for IEEE 802.16 (Yang et al., 2012; Yang et al., 2015a). LBPS mechanisms for UE power saving in LTE-FDD were also proposed

(Yang et al., 2015b). In order for the previously proposed schemes to be applied to LTE-TDD, the idea of virtual time is proposed in this paper. Mappings from virtual time to real time for different TDD configurations is also proposed. Performance benefit in terms of power saving efficiency is demonstrated by the simulation study.

The remainder of the paper is organized as follows. In section 2, a brief survey of the authors' previous work of LBPS is presented. Proposed schemes for power saving in LTE-TDD are presented in section 2. Performance evaluation is presented in section 4. Finally, section 5 concludes this paper.

## 2. Previous Work

The basic idea of LBPS is to take advantage of traffic modelling in determining the length of the sleep period. The traffic in LBPS is assumed to be Poisson process in order to take advantage of the multiplexing property. Taking a single UE with the downlink traffic as an example, the eNodeB estimates the traffic load and calculates the length of the sleep period in order for the accumulated data in the eNodeB's buffer reaching a predefined level as illustrated in Figure 1. The predefined level consists of two threshold parameters: *Data\_TH* and *Prob\_TH* as shown in Figure 1. The length of the sleep period is calculated by making the amount of accumulated data exceeding *Data\_TH* with probability higher than *Prob\_TH*.

The value of *Data\_TH* could be any value theoretically, but in practice it is suggested to set its value as the amount of data which can be served within the basic time unit of transmission scheduling (e.g. a *Transmission Time Interval* or subframe in LTE) in order to get a good balance between power saving and delay performance. In LTE, the amount of data which can be served in a subframe is fluctuated and affected by the link quality. In the authors' previous work (Yang et al., 2015b), *Channel Quality Indicator (CQI)* were used in estimating subframe capacity, and two types of CQI reporting namely *Wideband* reporting and *Full-Sub-band* reporting were addressed.

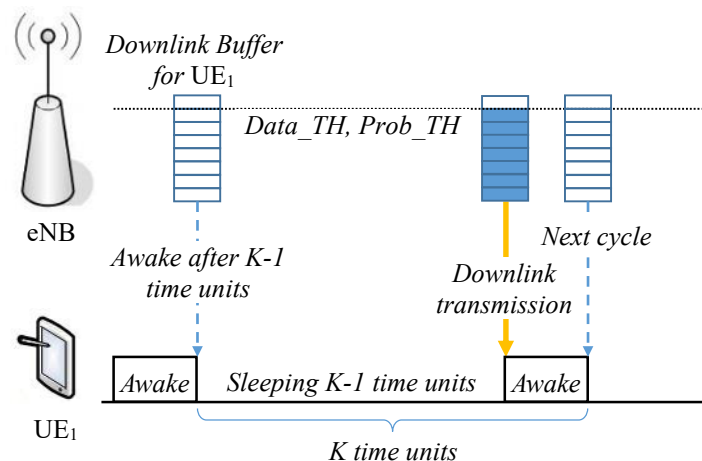
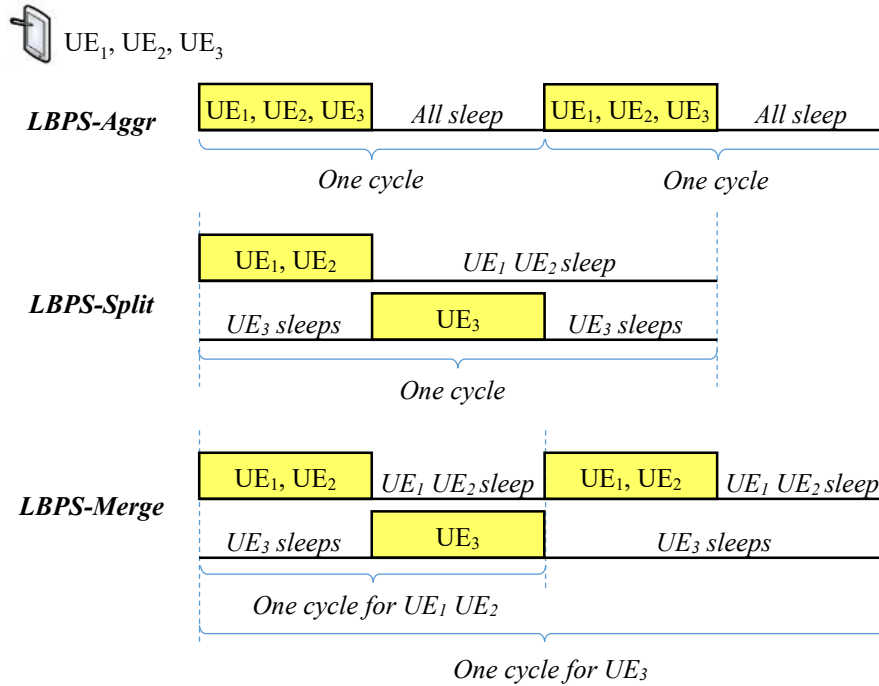


Figure 1. Load-Based Power Saving



**Figure 2. LBPS Schemes**

For the general case of multiple users in the network, three LBPS schemes namely *LBPS-Aggr*, *LBPS-Split*, and *LBPS-Merge* were proposed to deal with multiplexing users in sleep scheduling. *LBPS-Aggr* is the simplest scheme which treats all traffic as an aggregate flow in determining the length of the sleep period and synchronizes all UEs in sleep scheduling as illustrated in the upper part of Figure 2. The idea of *LBPS-Split* is motivated by the following observation on the sleep pattern of *LBPS-Aggr*. If we place the awake subframe of some UEs in a different part of a cycle, the cycle length could be extended since the load of each split group is less than the total load used in *LBPS-Aggr*. As illustrated in the middle part of Figure 2, a larger cycle is made by splitting UEs into two groups ( $UE_1+UE_2$  and  $UE_3$ ), resulting in better power saving performance.

*LBPS-Merge* is motivated by the idea that given a predefined level for data accumulation, the best case for a UE in terms of power saving is to make the UE a single-member group which results in the largest sleep period for the UE. Since different group in general has different cycle length, in order to efficiently find a feasible sleep schedule for all groups, the cycle length for each group in *LBPS-Merge* is converted to the closest and smaller power of 2. In the case that a feasible sleep schedule cannot be found for the current state of grouping, iterated merging operation of some groups is performed until a feasible sleep schedule is found. As illustrated in the lower part of Figure 2, there are two groups in the sleep schedule, the group of  $UE_1+UE_2$  with 2-subframe cycle and the group of  $UE_3$  with 4-subframe cycle.

### 3. Sleep Scheduling in LTE-TDD

#### 3.1 Basic idea

The LBPS schemes in the authors' previous work (Yang et al., 2015b) were originally designed for LTE-FDD. Although based on the general idea of data accumulation according to the estimated input load and the estimated capacity in a subframe, sleep scheduling in the schemes were assigned by assuming the availability of every subframe in a continuous manner. Two issues should be addressed in order to apply the LBPS schemes to LTE-TDD. Firstly, since the availability of subframe for DL data transmission in TDD depends on the given configuration, the algorithm of sleep scheduling needs to consider the pattern of available subframes. Secondly, the calculation of the estimated capacity for data accumulation needs to be revised, since the overall system capacity also depends on the TDD configuration.

There are two possible directions to design the algorithm of sleep scheduling in LTE-TDD. A straightforward way is to re-design a new set of schemes in order to accommodate different availability patterns of data transmission for different TDD configurations. However, this way would increase the complexity in sleep scheduling especially for a complicated scheme, such as *LBPS-Split* or *LBPS-Merge*, which adopts the mechanism of grouping UEs by splitting or merging.

Another direction is adopted by the authors to keep the previous LBPS schemes unchanged as much as possible and operate the schemes in the domain of *virtual time*, in which every subframe is continuously available for DL transmission. The result of sleep scheduling generated by the LBPS schemes in the domain of virtual time is then mapped to a sleep schedule in the domain of real time. Therefore, to apply LBPS schemes in LTE-TDD, the idea of virtual time associated with the mapping mechanisms from virtual time to real time for different TDD configurations is proposed in this paper. Mapping mechanisms for some of the configurations are presented in the next section, followed by the proposed sleep scheduling schemes in LTE-TDD.

#### 3.2 Mapping mechanisms

Although the system capacity depends on the channel quality, every subframe in virtual time is assumed to have the same amount of radio resource, which is allocated from the available radio resource in real time. Therefore, the design of the mapping mechanism for a given TDD configuration turns to be the problem of allocating available radio resource to each of the subframe in virtual time. Since this paper focuses on downlink traffic, the available radio resource for allocation is those subframes marked as "D" (for downlink transmission) in TDD configurations as displayed in Table 1. For the sake of simplicity, the special subframe (marked as "S") is not considered for downlink

transmission in the paper. Moreover, the capacity of each available subframe in real time is also assumed to be equal. A subframe in virtual time is called a virtual subframe and a subframe in real time is called a real subframe in the paper.

Taking *Configuration 1* (denoted by *CI*) as an explanatory example, there are three possible methods for allocating all available downlink radio resources to each virtual subframe in a cycle of 10ms, which is the length of a radio frame in LTE. The first method is called *One-to-All mapping*, denoted by *M1* in the paper, in which the radio resource for a virtual subframe comes from every available real subframe. As illustrated in Figure 3, there are 4 real subframes in a cycle of 10ms in *CI*. Each real subframe contributes 1/10 of its radio resource to each virtual subframe. In this way, each virtual subframe is with 4/10 of the capacity in a real subframe and maps to real subframe 0, 4, 5, and 9 in *M1*, which means an awake virtual subframe (e.g. virtual subframe 0) determined by the sleep scheduling scheme results in 4 awake real subframes (i.e. real subframe 0, 4, 5, 9). Apparently *M1* is not a good way of mapping from the viewpoint of power saving efficiency, thus it serves as a contrast to other mapping mechanisms.

Another method of mapping is called *Continuous mapping*, denoted by *M2*. In *M2*, as illustrated in Figure 4, starting from *real subframe 0* the available radio resource is first allocated to *virtual subframe 0* until reaching the equal share of the total capacity, i.e. 4/10 of the capacity in a real subframe in the case of *CI*. Another 4/10 of the capacity from *real subframe 0* is allocated to *virtual subframe 1*. The rest of 2/10 of the capacity from *real subframe 0* combined with 2/10 of the capacity from *real subframe 4* (the next available subframe in *CI*) is then allocated to *virtual subframe 2*. The rest of the radio resource from *real subframe 4* is allocated to *virtual subframe 3* and *virtual subframe 4*. The allocation process continues until all virtual subframes get their shares

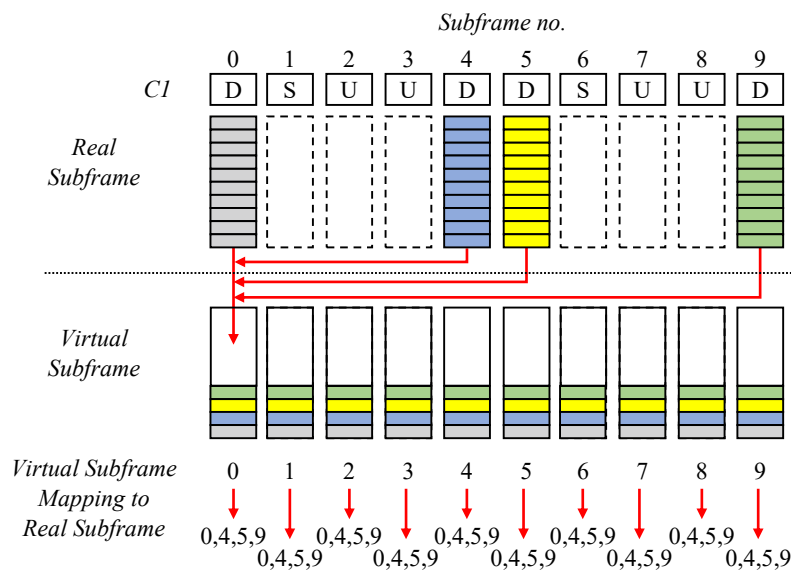


Figure 3. One-to-All mapping (M1) for CI

of the available radio resource. As displayed in the bottom part of Figure 4, there are only two cases of 1-to-2 mapping (1 virtual subframe mapping to 2 real subframes) in *M2*: virtual subframe 2 to real subframe 0 and real subframe 4, and virtual subframe 7 to real subframe 5 and real subframe 9. The rest of the mapping is all 1-to-1.

The third method is called *One-to-One first mapping*, denoted by *M3*. As illustrated in Figure 5, *M3* makes 1-to-1 mapping first and combines the rest of radio resource in real subframes for allocation. In this way, the type of 1-to-1 mapping from virtual to real (virtual subframe 0 ~ 7) goes first followed by the type of 1-to-2 mapping (virtual subframe 8~9) in *M3*. Moreover, as in *M2*, there are also two cases of 1-to-2 mapping in *M3*, and the difference is that the cases in *M3* are next to each other (virtual subframe 8 and 9).

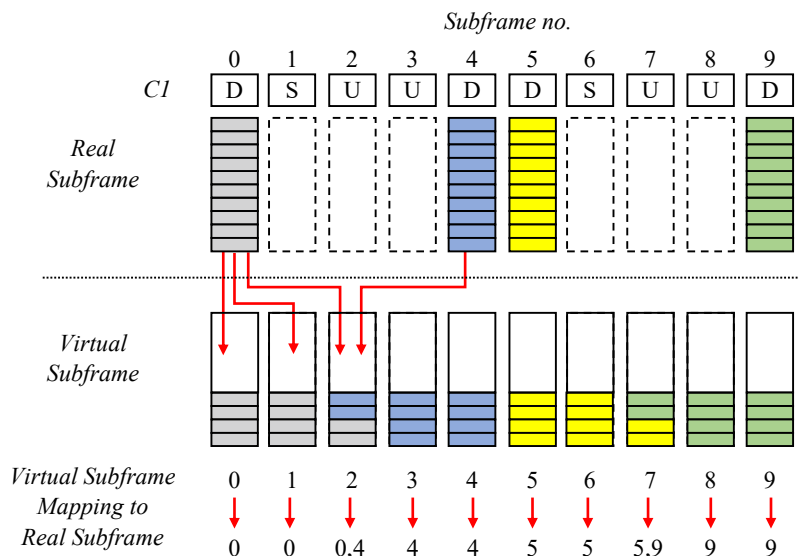


Figure 4. Continuous mapping (*M2*) for *CI*

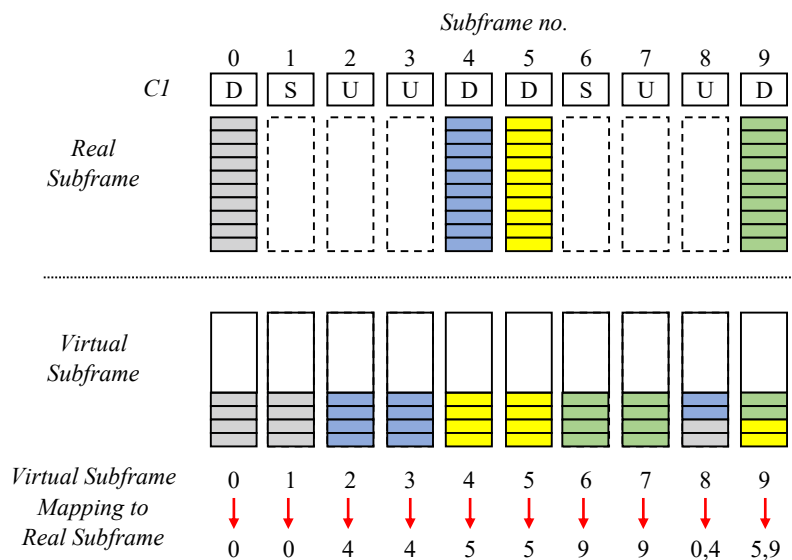


Figure 5. One-to-One first mapping (*M3*) for *CI*

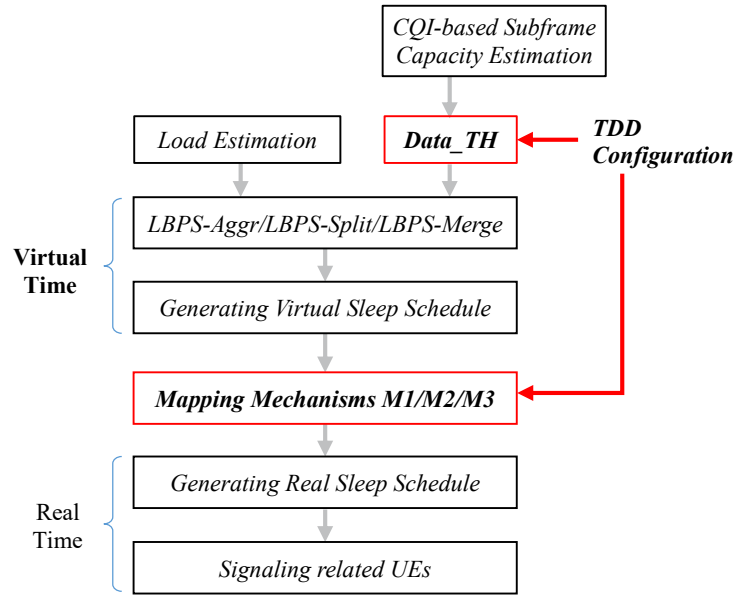
Table 2 displays *CI*'s three mappings, denoted by *C1M1*, *C1M2*, and *C1M3*. The entry in the row of a mapping in the table displays the real subframe number(s) to which the intended virtual subframe is mapping. For instance, the first entry of *C1M1* shows that *virtual subframe 0* maps to *real subframe 0, 4, 5, and 9*. The mappings for another two configurations, *C3* and *C5* are also included in the table. Note that a significant difference between *C5M2* and *C5M3* lies in the number of 1-to-many mapping. There are 6 cases of 1-to-2 mapping in *C5M2*. However, in *C5M3* except the two cases of 1-to-4 mapping, the rest is all 1-to-1. The impact of the number of 1-to-many mapping on the performance of power saving is investigated in Section 4.

Table 2. Mapping for *CI*, *C3*, and *C5*

Configuration Mapping	Subframe number									
	0	1	2	3	4	5	6	7	8	9
<i>C1</i>	D	S	U	U	D	D	S	U	U	D
<i>C1M1</i>	0,4 5,9	0,4 5,9	0,4 5,9	0,4 5,9	0,4 5,9	0,4 5,9	0,4 5,9	0,4 5,9	0,4 5,9	0,4 5,9
<i>C1M2</i>	0	0	0,4	4	4	5	5	5,9	9	9
<i>C1M3</i>	0	0	4	4	5	5	9	9	0,4	5,9
<i>C3</i>	D	S	U	U	U	D	D	D	D	D
<i>C3M1</i>	0, 5~9	0, 5~9	0, 5~9	0, 5~9	0, 5~9	0, 5~9	0, 5~9	0, 5~9	0, 5~9	0, 5~9
<i>C3M2</i>	0	0,5	5	5,6	6	7	7,8	8	8,9	9
<i>C3M3</i>	0	5	6	7	8	9	0,5	5,6	7,8	8,9
<i>C5</i>	D	S	U	D	D	D	D	D	D	D
<i>C5M1</i>	0, 3~9	0, 3~9	0, 3~9	0, 3~9	0, 3~9	0, 3~9	0, 3~9	0, 3~9	0, 3~9	0, 3~9
<i>C5M2</i>	0	0,3	3,4	4,5	5	6	6,7	7,8	8,9	9
<i>C5M3</i>	0	3	4	5	6	7	8	9	0, 3~5	6~9

### 3.3 Sleep scheduling

Proposed sleep scheduling for LTE-TDD in this paper is based on the previous work of LBPS and combined with the idea of virtual subframe as well as the mapping mechanism presented in the previous section. As illustrated in Figure 6, the value of *Data\_TH* is calculated according to the estimated capacity of a subframe and the given TDD configuration. *Data\_TH* and the estimated load are then fed into the sleep scheduling scheme to generate a virtual sleep schedule, which is further converted to a real sleep schedule by the mapping mechanism. Lastly, eNodeB notifies related UEs by transmitting the message of *RRC Connection Configuration*.



**Figure 6. LBPS schemes in LTE-TDD**

#### 4. Performance Evaluation

In this section, a performance comparison by theoretical analysis in terms of power saving efficiency for three different mapping mechanisms is presented, followed by the results of the simulation study.

##### 4.1 Analysis of the mapping mechanisms

In order to investigate the impact of the mapping mechanism on power saving, the case of  $PSE_{Virtual} = 0.9$  is analyzed, in which  $PSE_{Virtual}$  is defined as the average power saving efficiency ( $PSE$ ) in the domain of virtual time. In the case of  $PSE_{Virtual} = 0.9$ , it is assumed that there is only 1 awake virtual subframe within 10ms. Moreover, each virtual subframe in a radio frame is assumed to have the equal probability (i.e. 1/10) to be the awake subframe. Therefore, the average value of  $PSE$  in the domain of real time, denoted by  $PSE_{Real}$ , can be calculated as follows: (Note that  $sf$  is the abbreviation for subframe in the equation)

$$PSE_{Real} = \frac{1}{10} \sum_{i=0}^9 \left( 1 - \frac{\text{No. of mapped real sf for virtual sf } i}{10} \right)$$

The value of  $PSE_{Real}$  for  $PSE_{Virtual} = 0.9$  in different configurations and mappings is displayed in Table 3. Some observations can be made according to the table. First of all, the value of  $PSE_{Real}$  is smaller than  $PSE_{Virtual}$  (0.9) in all cases, since the case of 1-to-many mapping in the mapping mechanism is inevitable. Secondly, as expected, the method of  $M1$  mapping results in the smallest value of  $PSE_{Real}$ . Lastly, the same value of  $PSE_{Real}$  in  $M2$  and  $M3$  for a configuration implies that  $M2$  and  $M3$  have the similar power saving

performance. However, as will be demonstrated in the following sections of the simulation study,  $M3$  outperforms  $M2$  in most cases.

Table 3.  $PSE_{Real}$  for  $PSE_{Virtual} = 0.9$

Mapping	$PSE_{Real}$	Remarks
C1M1	0.6	$l-to-4 \times 10$
C1M2	0.88	$l-to-1 \times 8, l-to-2 \times 2$
C1M3	0.88	$l-to-1 \times 8, l-to-2 \times 2$
C3M1	0.4	$l-to-6 \times 10$
C3M2	0.86	$l-to-1 \times 6, l-to-2 \times 4$
C3M3	0.86	$l-to-1 \times 6, l-to-2 \times 4$
C5M1	0.2	$l-to-8 \times 10$
C5M2	0.84	$l-to-1 \times 4, l-to-2 \times 6$
C5M3	0.84	$l-to-1 \times 8, l-to-4 \times 2$

#### 4.2 Simulation environment and metrics

Three types of UEs are defined for simulating different cases of channel quality. An  $H$ -type (high link quality) UE is assumed to use 64QAM modulation with CQI value ranging from 10 to 15. An  $M$ -type (medium link quality) UE uses 16QAM with CQI ranging from 7 to 9. An  $L$ -type (low link quality) UE uses QPSK with CQI ranging from 1 to 6. In addition to the three proposed schemes, a contrast scheme based on standard DRX (denoted by *Std. DRX*) is also simulated. Parameters used in the simulation are summarized in Table 4.

Table 4. Simulation Parameters

Channel capacity	20 MHz (#RB = 100)
# UE	40 (equal load)
Type of UE	$H$ -type: CQI 10~15 $M$ -type: CQI 7~9 $L$ -type: CQI 1~6
Packet Size	799 bits
$DATA\_TH$	Estimated Capacity $\times$ 0.8
$Prob\_TH$	0.8
Min. Group Size	1

Contrast scheme <i>Std. DRX</i>	On duration = 1ms Inactivity timer = 10ms Short DRX Cycle = 40ms Short Cycle timer = 2 Long DRX Cycle = 160ms
------------------------------------	---

The performance metric investigated in the simulation study is *Power Saving Efficiency*, denoted by *PSE*, which is defined as the ratio of time in the sleep mode.

### 4.3 Simulation results

Figures 7~9 display the results of *PSE* for different mappings in the scheme of *LBPS-Aggr* with *All-H* type UEs. In the figures there are two rows of index for the x-axis. The upper row is the input load  $\lambda$  in Mbps, the lower row is the normalized utilization  $\rho$  calculated as dividing the input load by the average system capacity. As expected, the mapping of *M1* results in the worst *PSE* among the mapping mechanisms.

On the other hand, although with the same analytical *PSE* result (Table 3) and similar simulation results for  $\rho=0.1$ , *M3* outperforms *M2* in most of the load cases. The reason lies in the assumption of the equal probability for each subframe to be the awake subframe in the analysis. The equal probability assumption holds for the light load of  $\rho=0.1$ , which is demonstrated by the simulation results. However, the assumption no longer holds when  $\rho$  is larger than 0.1 and in most of the cases the clustering behavior of 1-to-many mappings in *M3* creates more benefit than the scattering style of *M2* in terms of *PSE*.

Figures 10~12 display the results of *PSE* for different schemes with *All-H* type UEs using the mapping of *M3*. The figures shows that in terms of *PSE* the schemes of *LBPS-Split* and *LBPS-Merge* outperform the scheme of *LBPS-Aggr*, which outperforms the contrast scheme of *Std. DRX*, demonstrating the benefit of the proposed schemes in power saving.

In order to investigate the impact of the sleep scheduling mechanism on delay performance, Figures 13~15 display the average access delay of the proposed schemes as well as the contrast scheme. The figures show that under light load and medium load ( $\rho=0.1\sim 0.6$ ) the scheme achieving high power saving efficiency, such as *LBPS-Split* and *LBPS-Merge*, results in higher access delay (e.g. larger than 50ms for the very light load of  $\rho=0.1$ ), which may not be acceptable for real-time traffic.

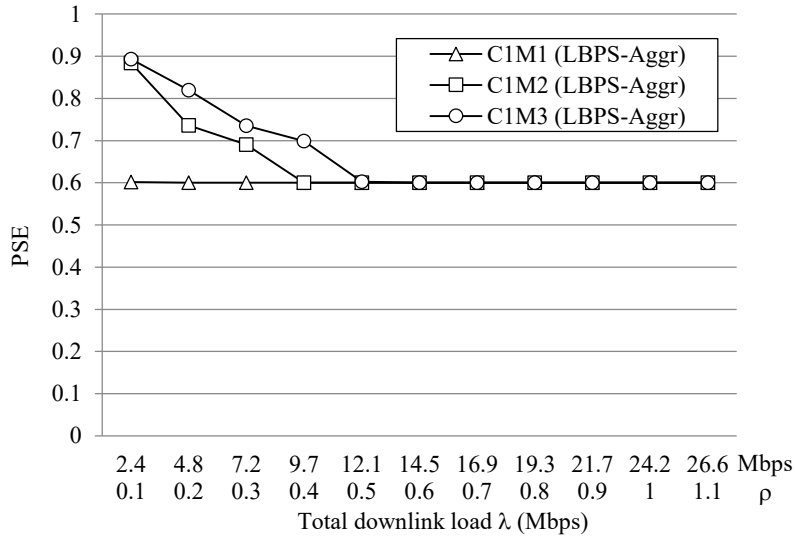


Figure 7. PSE of different mapping for C1 (All-H UEs)

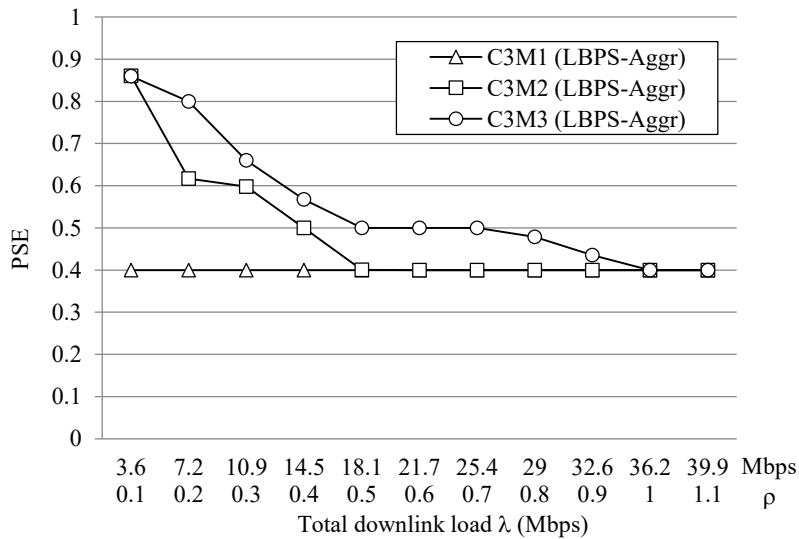


Figure 8. PSE of different mapping for C3 (All-H UEs)

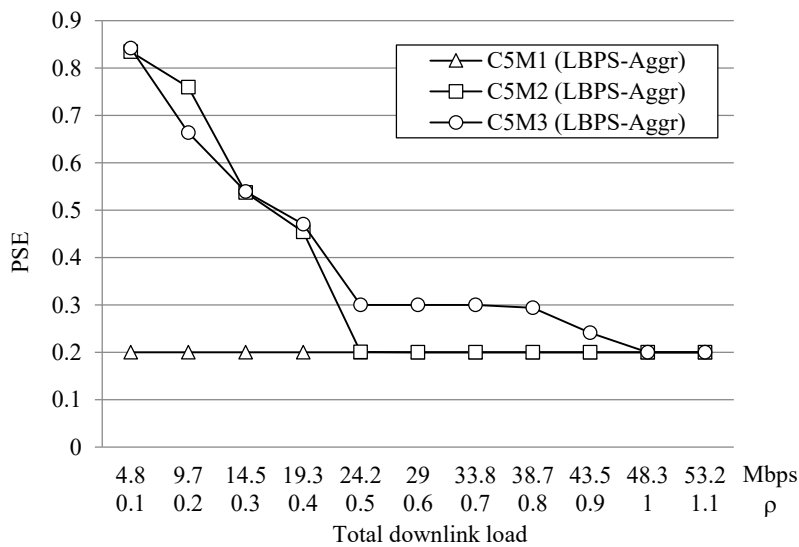


Figure 9. PSE of different mapping for C5 (All-H UEs)

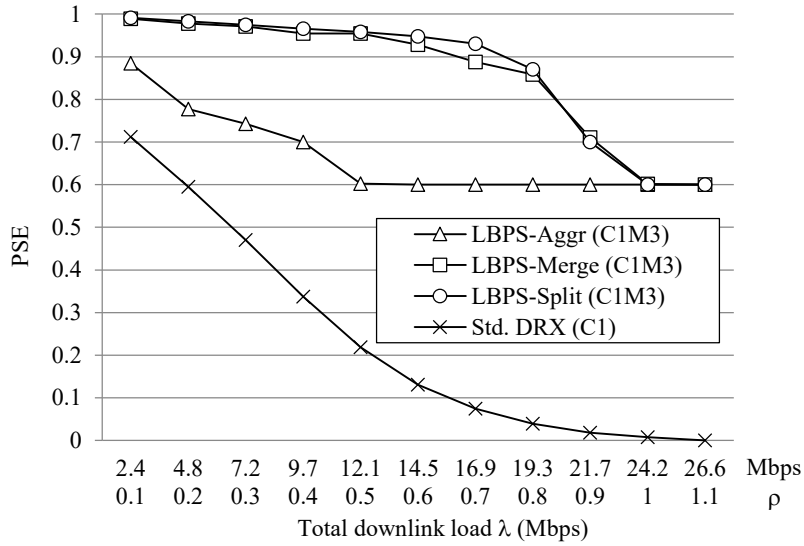


Figure 10. PSE of different schemes for C1 (All-H UEs)

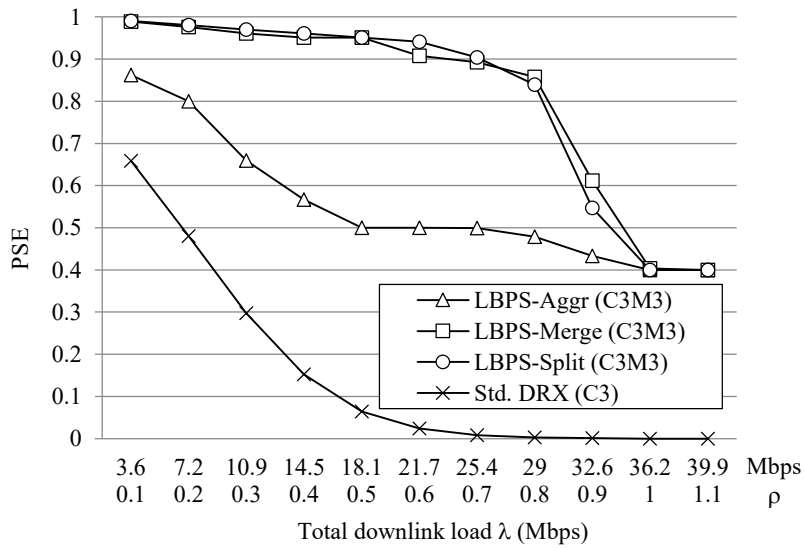


Figure 11. PSE of different schemes for C3 (All-H UEs)

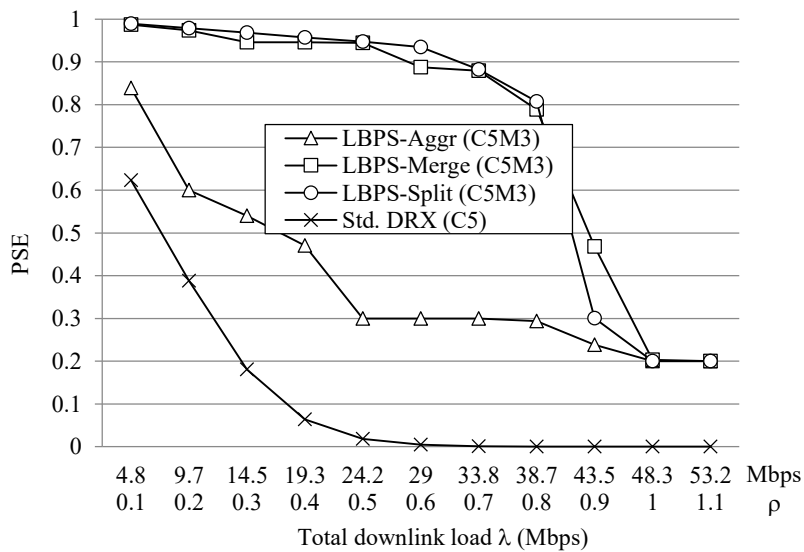


Figure 12. PSE of different schemes for C5 (All-H UEs)

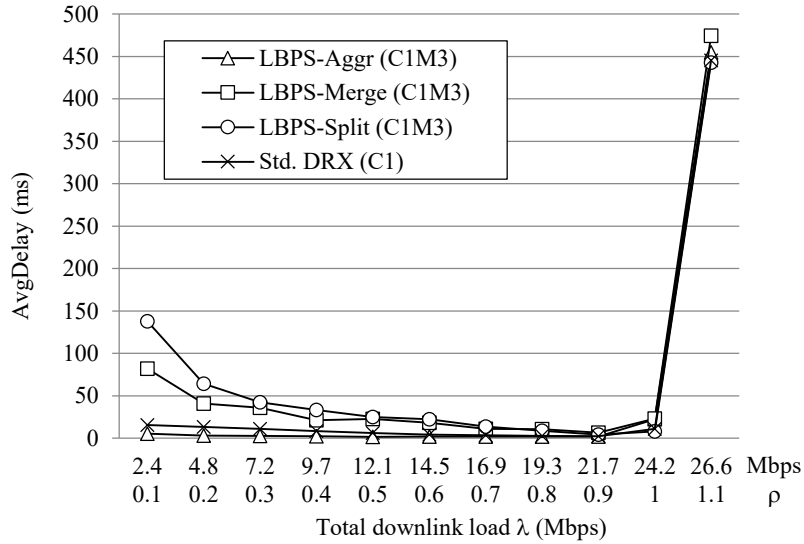


Figure 13. Average Delay of different schemes for C1 (All-H UEs)

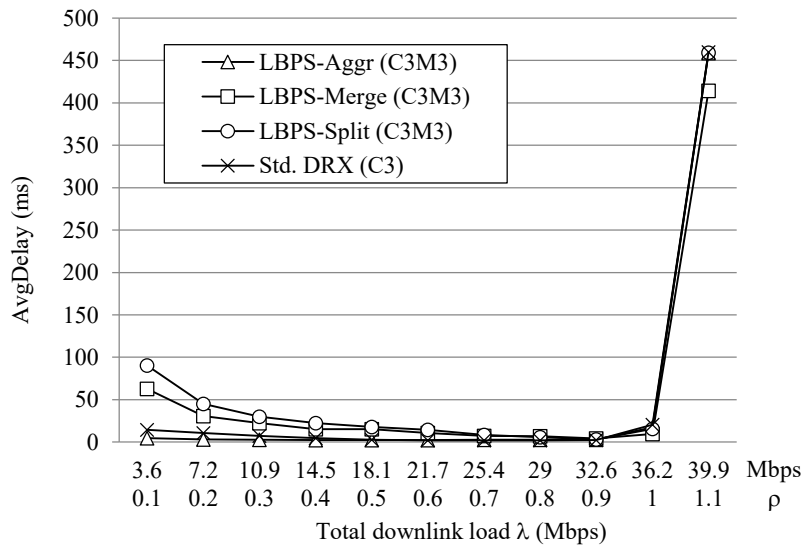


Figure 14. Average Delay of different schemes for C3 (All-H UEs)

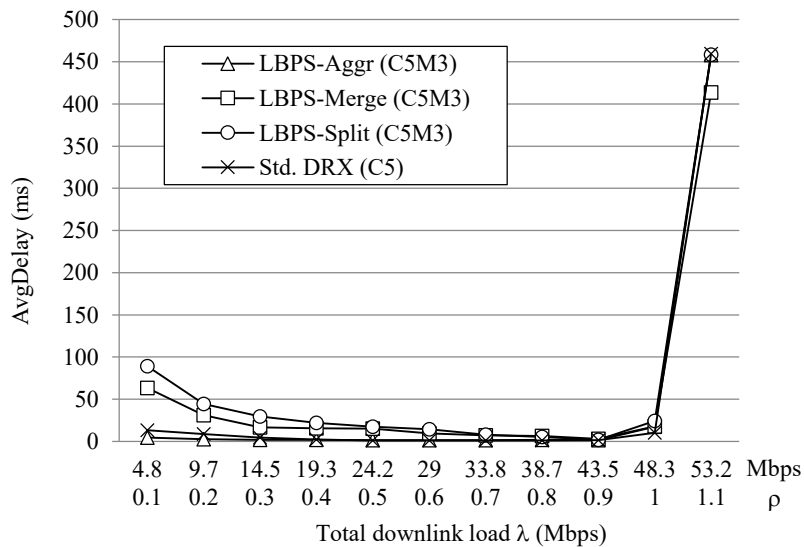


Figure 15. Average Delay of different schemes for C5 (All-H UEs)

## 5. Conclusion

The issue of energy saving in modern communication system has long been an important research topic in the literature. The authors previously proposed the idea of *Load-Based Power Saving (LBPS)* and three *LBPS* schemes, namely *LBPS-Aggr*, *LBPS-Split*, and *LBPS-Merge* for the mode of frequency division duplex (FDD) in LTE. In this paper, the applicability of the previously proposed schemes to the mode of time division duplex (TDD) in LTE is investigated. The idea of virtual time associated with the mapping mechanism from virtual time to real time in sleep scheduling is proposed. The following three types of mapping strategy are proposed in this paper: *One-to-All mapping (M1)*, *Continuous mapping (M2)*, and *One-to-One first mapping (M3)*. Simulation study shows that *M3* outperforms the other two in terms of power saving efficiency. With the mapping mechanisms for different TDD configurations, the three *LBPS* schemes can be applied to LTE-TDD and as demonstrated by the simulation study, better power saving performance than the standard-based mechanism can be achieved by the proposed schemes.

## ACKNOWLEDGEMENTS

This work was supported in part by the Ministry of Science and Technology, Taiwan, R.O.C., under grant no. MOST 104-2221-E-260-024.

## REFERENCES

- 3GPP. 2008. TS 36.300, "Evolved Universal Terrestrial Radio Access (E-UTRA) and Evolved Universal Terrestrial Radio Access Network (E-UTRAN)," Rel. 8, v8.5.0, May 2008.
- 3GPP. 2011. TS 36.300, "Evolved Universal Terrestrial Radio Access (E-UTRA) and Evolved Universal Terrestrial Radio Access Network (E-UTRAN)," Rel. 10, v10.3.0, March 2011.
- Brown, J., and Khan, J. Y. 2012. Performance analysis of an LTE TDD based smart grid communications network for uplink biased traffic, *Proceedings of Globecom Workshops*, Anaheim, CA, 3-7 Dec. 2012.
- Ji, H., Kim, Y., Choi, S., Cho, J., and Lee, J. 2013. Dynamic Resource Adaptation in Beyond LTE-A TDD Heterogeneous Networks, *Proceedings of IEEE International Conference on Communications (ICC)*, Budapest, 9-13 June 2013.
- Li, Y., Lin, Z., Liu, H., Gao, Y., Zhang, X., and Liu, X. 2014. Performance Evaluation of a Resource Allocation Scheme for Mixed Traffic in Dynamic-TDD Network, *Proceedings of the 80<sup>th</sup> IEEE Vehicular Technology Conference (VTC Fall)*, Vancouver, BC, 14-17 Sept. 2014.
- Lu, Y., Liu, L., Li, M., and Chen, L. 2012. Uplink Control for Low Latency HARQ in

- TDD Carrier Aggregation, *Proceedings of the 75<sup>th</sup> IEEE Vehicular Technology Conference (VTC Spring)*, Yokohama, 6-9 May 2012.
- Sheu, S. T., Kuo, K. H., Yang, C. C., and Sheu, Y. M. 2013. A Go-back-N HARQ Time Bundling for Machine Type Communication Devices in LTE TDD, *Proceedings of IEEE Wireless Communications and Networking Conference (WCNC)*, Shanghai, 7-10 Apr. 2013.
- Wang, C., Hou, X., Harada, A., Yasukawa, S., and Jiang, H. 2014. HARQ Signalling Design for Dynamic TDD System, *Proceedings of the 80<sup>th</sup> IEEE Vehicular Technology Conference (VTC Fall)*, Vancouver, BC, 14-17 Sept. 2014.
- Yang, C. C., Mai, Y. T., Chen, J. Y., Shen, Y. S., and Kuo, Y. C. 2012. LBPS: Load-based Power Saving in the IEEE 802.16e Network, *Computers and Electrical Engineering*, 38 (4), 891-905.
- Yang, C. C., Mai, Y. T., Chen, J. Y., and Kuo, Y. C. 2015. Integrated Load-based Power Saving for BS and MSS in the IEEE 802.16e Network, *Wireless Communications and Mobile Computing*, 15 (4), 601-614.
- Yang, C. C., Chen, J. Y., Mai, Y. T., and Liang, C. H. 2015. Adaptive Load-based and Channel-aware Power Saving for Non-Real-Time Traffic in LTE, *EURASIP Journal on Wireless Communications and Networking*, 2015 (1).